Evaluation of the mechanical properties of microarc oxidation coatings and 2024 aluminium alloy substrate

2002 J. Phys.: Condens. Matter 14 10947

(http://iopscience.iop.org/0953-8984/14/44/407)

INSTITUTE OF PHYSICS PUBLISHING JOURNAL OF PHYSICS: CONDENSED MATTER

J. Phys.: Condens. Matter **14** (2002) 10947–10952 PII: S0953-8984(02)37504-0

Evaluation of the mechanical properties of microarc oxidation coatings and 2024 aluminium alloy substrate

Wenbin Xue[1], **Chao Wang**[1], **Zhiwei Deng**[1,2], **Ruyi Chen**[1], **Yongliang Li**[2] **and Tonghe Zhang**[1]

[1] Key Laboratory for Radiation Beam Technology and Materials Modification, Institute of Low Energy Nuclear Physics, Beijing Normal University, Beijing, 100875, China

[2] Analytical and Testing Centre, Beijing Normal University, Beijing, 100875, China

E-mail: xuewb@263.net

Received 29 May 2002
Published 25 October 2002
Online at stacks.iop.org/JPhysCM/14/10947

Abstract

A determination of the phase constituents of ceramic coatings produced on Al–Cu–Mg alloy by microarc discharge in alkaline solution was performed using x-ray diffraction. The profiles of the hardness, H, and elastic modulus, E, across the ceramic coating were determined by means of nanoindentation. In addition, a study of the influence of microarc oxidation coatings on the tensile properties of the aluminium alloy was also carried out. The results show that the H- and E-profiles are similar, and both of them exhibit a maximum value at the same depth of coating. The distribution of the α-Al_2O_3 phase content determines the H- and E-profiles of the coatings. The tensile properties of 2024 aluminium alloy show less change after the alloy has undergone microarc discharge surface treatment.

1. Introduction

Microarc oxidation (MAO) is an unconventional plasmachemical–electrochemical method of forming ceramic coatings on valve metals such as Al, Mg, Ti [1–5]. During oxidation, many visible spark or microarc spots of several microns move rapidly on the metal surface in aqueous solution. The local instantaneous temperature and pressure inside these microarc discharge channels can reach 10^3–10^4 K and 10^2–10^3 MPa, respectively [6]. In the process of MAO, the Al substrate is directly oxidized to become α-Al_2O_3 and γ-Al_2O_3 phases due to a high-temperature sintering in the microarc zone. So there is an ideal adhesion between the MAO coating and the metal substrate. The surface properties of the Al alloys, such as wear resistance, corrosion resistance, high-temperature shock, electrical insulation, can be surprisingly improved [7–9]. Applications are expected in many fields.

In this work, a determination of the phase composition of MAO ceramic coatings on 2024 Al–4.3Cu–1.5Mg alloy was performed using x-ray diffraction (XRD). The distributions of the

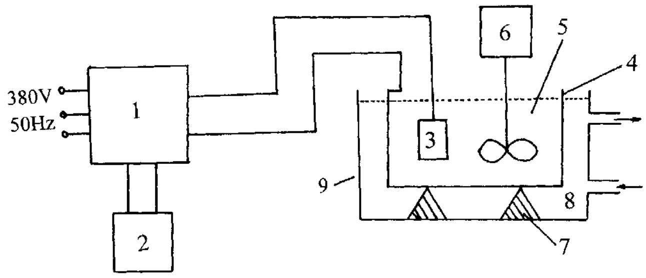

Figure 1. A schematic diagram of the 30 kW ac MAO system: 1, high-voltage power supply; 2, controlling system; 3, sample; 4, stainless steel bath; 5, aqueous solution; 6, stirring system; 7, partition insulator; 8, cooling water; 9, plastic bath.

hardness, H, and elastic modulus, E, across the ceramic coating were determined by means of nanoindentation. In addition, investigations of the tensile properties of the aluminium alloy before and after surface treatment by MAO were carried out.

2. Experimental procedure

In the experiment, the ceramic coating was accomplished with a home-made ac MAO system. As shown in figure 1, the system consists of a potential adjustable ac power supply, up to 1000 V, a stainless steel container used as an electrolyte cell, and a stirring system and cooling system. The sample and container wall were used as two electrodes, respectively. Disks of Al–4.3Cu–1.5Mg 2024 alloy, 40 mm × 7 mm, were used as the primary samples. Furthermore, some standard tensile samples were studied. The electrolyte was an alkaline solution.

After MAO, the discs were cut and the metallographic specimens were prepared. The microstructure and phase composition in a cross-sectional specimen were analysed by means of SEM and XRD. Nanohardness and elastic modulus measurements of the MAO coating and alloy substrate were performed using a mechanical properties microprobe (Nano Indenter II, manufactured by Nano Instruments, Inc.) with load and displacement resolutions of 75 nN and 0.04 nm, respectively [10]. Also, tensile samples with different coating thicknesses were prepared, and then the studies of the tensile properties were carried out using a MTS-810 materials tester.

3. Results and discussion

3.1. Microstructure and phase constituents of the ceramic coatings on 2024 aluminium alloy

Figure 2 is a SEM micrograph of the ceramic coatings obtained with Al line scanning. The coating/substrate interface is clear, and no big voids can be observed near the interface. The alumina ceramic coating was 230 μm thick, which is much thicker than anodic oxide on aluminium alloy. Furthermore, the coating actually contains a loose surface layer and compact layers 60 and 170 μm thick. The compact layer is very dense and pores are hardly observed.

XRD analysis shows that the MAO coating on 2024 Al alloy is mainly composed of α-Al_2O_3 and γ-Al_2O_3 phases. With C_α and C_γ representing the relative contents of the α-Al_2O_3 and γ-Al_2O_3 phases ($C_\alpha + C_\gamma = 1$), figure 3 depicts the distribution of the α-Al_2O_3 content C_α along the coating depth. By comparing figures 2 and 3, we see that the loose layer consists of about 88 wt% of α-Al_2O_3 phase and about 12 wt% of γ-Al_2O_3 phase. The

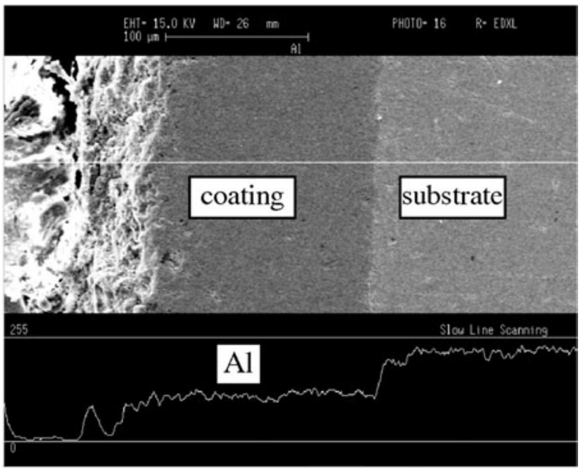

Figure 2. A cross-sectional micrograph of the MAO coating on 2024 Al alloy with Al line scanning.

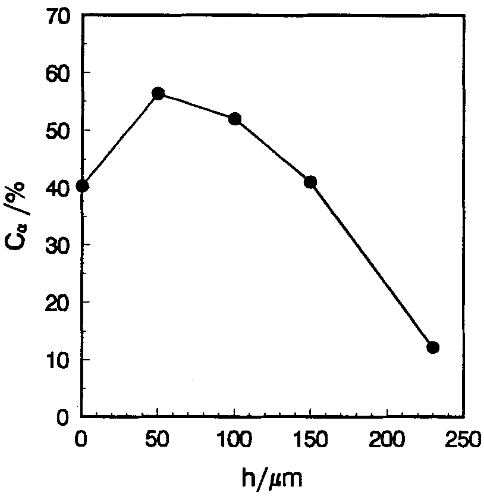

Figure 3. The distribution of the α-Al_2O_3 content C_α through the depth of the coating formed on 2024 Al alloy by MAO.

contents in the compact layer are approximately 50 wt% respectively. From the surface layer to the interior of the MAO coating, C_α gradually increases while C_γ reduces. However, C_α at 50 μm depth from the Al/Al_2O_3 interface reaches a maximum value; then it decreases near the interface.

3.2. *Nanoindentation test*

As shown in figure 4, the nanohardness (H) and elastic modulus (E) in the compact layer of the MAO coating on 2024 aluminium alloy are in the ranges of 18–32 and 280–390 GPa, respectively. The curve profiles of the H- and E-distributions are very similar. From the Al/Al_2O_3 interface to the outer layer of the coating, H and E first increase gradually with

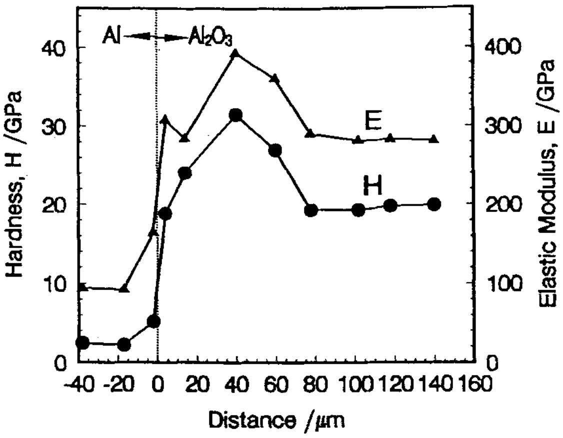

Figure 4. Profiles of nanohardness, H, and elastic modulus, E, for the MAO coating and 2024 Al alloy substrate under a 50 mN load.

Table 1. Tensile properties of the 2024 aluminium alloy treated by MAO.

Sample	Thickness (μm) Unpolished	Thickness (μm) Polished	σ_s (MPa)	σ_b (MPa)	δ (%)	ψ (%)	E (GPa)
O	0		420	580	15	14.0	72
A	60		415	560	13	17.0	71
B	100		415	560	14	17.0	71
C	160		410	550	12	19.5	70
A1		40	415	560	13	15.5	72
B1		60	415	570	14	14.0	71
C1		100	415	560	14	18.0	71

distance, then both of them reach maximum values at the same distance of 40 μm from the interface. After reaching the maximum values, they begin to decrease with distance. In the region of 80–140 μm, H and E show approximately no change. Comparing figure 4 with figure 3, it seems that the distribution of α-Al_2O_3 phase content determines the H- and E-profiles of the coatings.

3.3. Influence of MAO on tensile properties of the alloy substrate

In table 1, sample O is an untreated aluminium alloy sample. After samples A, B, and C were ground with SiC paper, the remaining coating thicknesses were 40, 60, 100 μm, respectively; these samples are labelled A1, B1, C1. Note that every data value in the table represents an average over the same three samples.

As shown in table 1, the tensile properties of 2024 aluminium alloy show less change after the alloy has undergone MAO surface treatment. For the samples A, B, C with different coating thicknesses, the decreases of the yield strengths (σ_s), tensile strengths (σ_b), and elastic moduli (E) are less than 5% relative to the those of the untreated sample O, and the contractions of the area (ψ) show less increase while the elongations (δ) slightly decrease. After the loose layers of the oxide coatings are polished, the improvements in the tensile properties of the alloy are also less marked, especially for these samples with less coating thickness. These

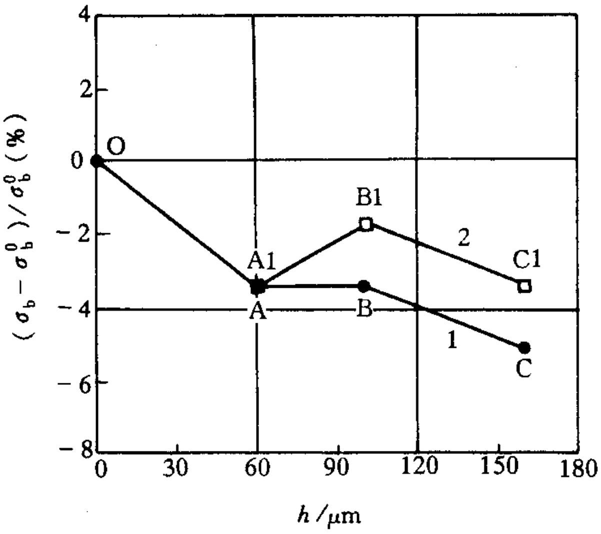

Figure 5. The effect of coating thickness h on the tensile strength σ_b of 2024 aluminium alloy. σ_b^0 is the tensile strength of the unoxidized sample. 1: unpolished; 2: polished coating.

conclusions are clearly apparent in figure 5 which shows the tensile strength change with the coating thickness. Hence, after MAO treatment, the surface properties of aluminium alloy can be significantly improved; however, its tensile properties can be almost unchanged. This is very advantageous for industrial applications of MAO technology.

In addition, SEM observation indicates that many fragments of the oxide coatings remain uniformly on the surfaces of the tensile samples, which identifies that the adhesion between the oxide coating and alloy is excellent.

4. Conclusions

(1) The ceramic coatings formed on 2024 aluminium alloy by MAO consist of two layers, a loose layer and a compact layer. The nanohardness, H, and elastic modulus, E, of the compact layer are 18–32, 280–390 GPa, respectively. The H- and E-profiles of the coatings are similar. Each of them has a maximum value at the same depth of coating.

(2) The distribution of the α-Al_2O_3 phase content in the coatings also has a maximum value, and it determines the H- and E-profiles.

(3) The tensile properties of 2024 aluminium alloy show smaller change after the alloy has undergone MAO surface treatment. For all samples with different thicknesses of coating, the decreases of the yield strengths, tensile strengths, and elastic moduli are below 5%, and the contractions of area show less increase while the elongations slightly decrease. After the oxide coatings are polished, the improvements in the tensile properties of the alloy are also rather small.

Acknowledgments

This work was supported by the National ‘863’ High-Tech Program of China (715-011-020), the National Natural Science Foundation of China (59801003) and Beijing New-Star Program for Science and Technology (9558102500).

References

[1] Van T B, Brown S D and Wirtz G P 1977 *Am. Ceram. Soc. Bull.* **56** 563
[2] Xue W, Deng Z, Lai Y and Chen R 1998 *J. Am. Ceram. Soc.* **81** 1365
[3] Xue W, Deng Z, Chen R and Zhang T 2000 *Thin Solid Films* **372** 114
[4] Xue W, Deng Z, Chen R and Zhang T 2000 *Surf. Eng.* **16** 344
[5] Yerokhin A L, Lyubimov V V and Ashitkov R V 1998 *Ceram. Int.* **24** 1
[6] Klapkiv M D 1995 *Mater. Sci.* **31** 494
[7] Slonova A I, Terleeva O P, Shulepko E K and Markov G A 1992 *Elektrochimiya* **28** 1280
[8] Timoshenko A V and Magurova Yu V 1995 *Zashch. Met.* **31** 523
[9] Nie X, Leyland A, Song H W, Yerokhin A L, Dowey S J and Matthews A 1999 *Surf. Coat. Technol.* **116** 1055
[10] Bolshakov A and Pharr G M 1998 *J. Mater. Res.* **13** 1049